

# Effects of Crosstalk in WDM Optical Label Switching Networks Due to Wavelength Switching of a Tunable Laser

F. Smyth, *Student Member, IEEE*, E. Connolly, *Student Member, IEEE*, A. K. Mishra, A. D. Ellis, D. Cotter, A. Kaszubowska, *Member, IEEE*, and L. P. Barry, *Member, IEEE*

**Abstract**—Crosstalk caused by switching events in fast tunable lasers in an optical label switching (OLS) system is investigated for the first time. A wavelength-division-multiplexed OLS system based on subcarrier multiplexed labels is presented which employs a 40-Gb/s duobinary payload and a 155-Mb/s label on a 40-GHz subcarrier. Degradation in system performance as the transmitters switch between different channels is then characterized in terms of the frequency drift of the tunable laser.

**Index Terms**—Fast tunable laser, optical label switching (OLS), optical packet switching (OPS), subcarrier multiplexed (SCM) label.

## I. INTRODUCTION

OPTICAL packet switching (OPS) networks employing optical label switching (OLS) techniques can offer high bandwidth efficiency, good scalability, and fast reconfigurability [1], [2]. In an OPS network, when electrical data packets from the client networks arrive at the “ingress” node, the Internet protocol (IP) header is examined and a label and wavelength are computed based on the destination of the packet. The packet has its newly computed label attached and is transmitted using a fast tunable laser into the network on the appropriate optical wavelength. At each node, a routing decision is made based on the label, and by switching another fast tunable laser, the packet can be shifted to a new wavelength using, for example, a semiconductor optical amplifier (SOA)-based wavelength converter [3], [4]. On reaching the other side of the core network, the label is removed at the “egress” node and the original packet is routed as normal using electrical routing hardware.

Optical subcarrier multiplexed (SCM) labels are one of the possible solutions for label coding [5]–[7]. The label data is placed on a radio-frequency subcarrier and used to intensity modulate the laser resulting in two sidebands containing the label information, centered on the optical carrier, which contains the payload data. The SCM label can be read by detecting the entire multiwavelength signal and then downconverting the label [8], or by extracting the label using an optical bandpass

Manuscript received May 15, 2006; revised August 1, 2006. This work was supported by Science Foundation Ireland through the Investigator Program and by the Centre for Telecommunications Value Chain Research (CTVR).

F. Smyth, E. Connolly, A. Kaszubowska, and L. P. Barry are with the Research Institute for Networks and Communications Engineering, Dublin City University, Glasnevin, Dublin 9, Ireland (e-mail: smythf@ceeng.dcu.ie).

A. K. Mishra, A. D. Ellis, and D. Cotter are with the Tyndall National Institute, “Lee Maltings”, Cork, Ireland (e-mail: arvind.mishra@ucc.ie).

Digital Object Identifier 10.1109/LPT.2006.883888

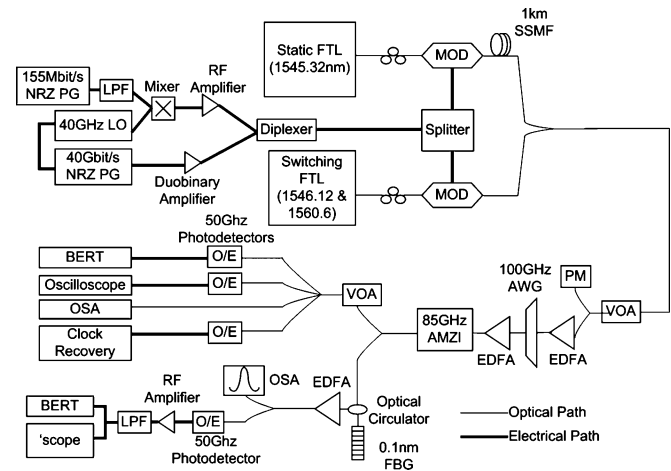


Fig. 1. Experimental setup employing two fast tunable lasers (FTLs).

filter and detecting it directly [9]. The advantages of SCM labels over the other methods are that they are very easily generated and detection is simple. Also, there are no strict timing and synchronisation requirements. However, the technique is less spectrally efficient than other methods and SCM labels suffer both from dispersion-induced fading, and from intermodulation distortion, which can lead to degradation of the labels.

In this letter, we investigate interference in a two-channel OLS system caused by the wavelength drift of the tunable laser in the packet transmitter as it tunes between different output wavelengths. These effects are examined and characterized as a function of the wavelength drift of the tunable laser.

## II. EXPERIMENTAL SETUP

The experimental setup is shown in Fig. 1. The two laser transmitters used were fast tunable lasers based on sampled grating distributed Bragg reflector technology [10] that can switch between every  $C$ -band channel on the 50-GHz spacing ITU grid.

An SOA at the output of the lasers allowed the light to be “blanked” to prevent spurious output as the laser transitions from one channel to another. The laser transmitters were both modulated with a data signal which consisted of 40-Gb/s duobinary baseband data combined with a 40-GHz subcarrier modulated with 155-Mb/s data. The payload drive voltage to each modulator was approximately  $0.9 V\pi$ . The peak-to-peak drive amplitude of the subcarrier was less than  $0.5 V\pi$ . The use of the duobinary coding for the payload, previously used to increase the spectral efficiency of a packet routing system [11], ensured

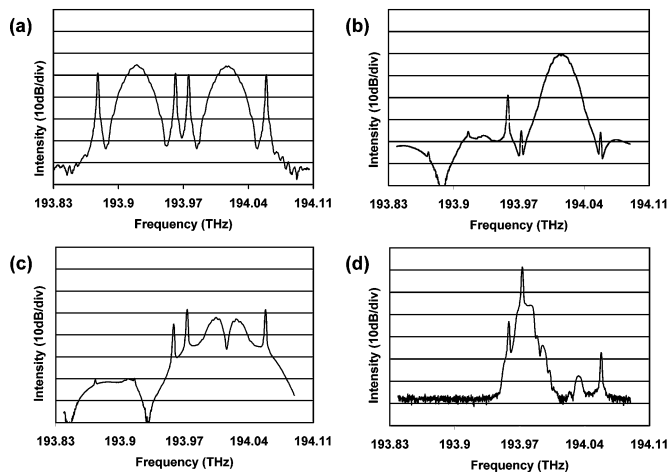


Fig. 2. Spectra at different stages of the system. (a) Two channels 100 GHz apart; (b) suppressed labels at one port of AMZI; (c) suppressed payload at second port of AMZI; (d) extracted label.

minimal spectral overlap between payload and label. While the use of independent modulators in series for label and payload modulation would require a compromised payload extinction ratio to avoid degradation of the label, the use of a single modulator ensures that a subcarrier signal is always present, albeit somewhat amplitude modulated by the payload data.

Before coupling the two channels together, one of them was passed through 1 km of optical fiber in order to decorrelate the data patterns. This corresponded to six word lengths for the label and 15 625 word lengths for the payload.

Fig. 2(a) shows the input spectrum to the receiver, with both lasers operating in continuous-wave mode. The signal was pre-amplified and the 194-THz channel was selected using a 100-GHz Gaussian profiled arrayed waveguide grating (AWG) with a 3-dB bandwidth of 65 GHz. Another erbium-doped fiber amplifier was then used to boost the signal before filtering it with an asymmetric Mach-Zehnder interferometer (AMZI) with an FSR of 85 GHz. The signals at the output ports of the AMZI are shown in Fig. 2(b) and (c). In Fig. 2(b), approximately 30-dB suppression is shown on the extracted channel's labels at the payload port, and in Fig. 2(c), a suppression of approximately 10 dB of the payload is shown at the labels port.

In the label receiver, the input arm of a circulator was connected to a tunable fiber Bragg grating with a 3-dB reflection bandwidth of approximately 12 GHz. This bandwidth is wide enough to ensure correct detection of the label even in the case of wavelength drift of the tunable laser. The filter was tuned to reflect the left-hand label of the extracted channel. The reflected label [Fig. 2(d)] was directly detected, electrically amplified, and low-pass filtered. The output of the receiver was split electrically and passed into the bit-error-rate (BER) tester and oscilloscope.

### III. RESULTS AND DISCUSSION

Initially we looked at the effects that the label and payload have on each other in a simple single-channel system. The pattern length of both the payload and label was  $2^7 - 1$ . In Fig. 3(a) ( $\circ$  and  $\triangle$ ), it is shown that the presence of the label barely affected the payload at all. However, the presence of the duobinary payload had a detrimental effect on the label introducing

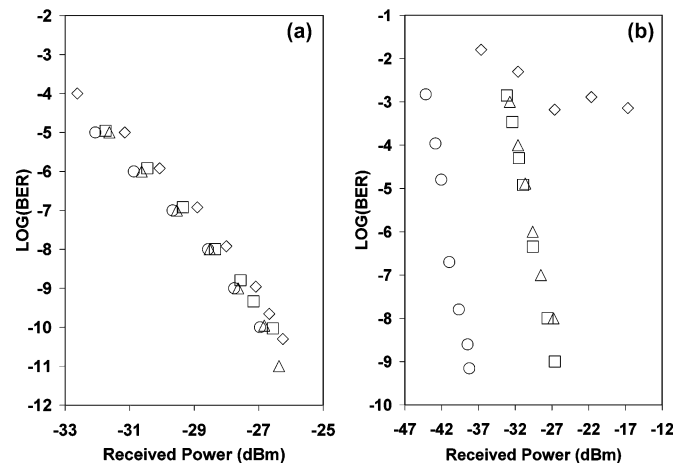


Fig. 3. (a) BER of the 194-THz channel *payload* versus received power in one channel for four cases: single channel without label ( $\circ$ ); single labelled channel ( $\triangle$ ); two static labelled channels ( $\square$ ); two switching labelled channels ( $\diamond$ ). (b) BER of the 194-THz channel *label* versus received power in one channel for four cases: single label without payload ( $\circ$ ); single channel label with payload present ( $\triangle$ ); two static channels ( $\square$ ); two switching channels ( $\diamond$ ).

a power penalty of approximately 13 dB. This can be seen in Fig. 3(b) ( $\circ$  and  $\triangle$ ). Of this label penalty, 11.4 dB were attributable to the power distribution between the payload (93%) and label (7%). The remaining 1.6-dB penalty was attributed to the aggregate modulation of the bias position of the 40-GHz subcarrier by the payload data (averaged over 258 bits). Owing to the low label signal amplitude, this pattern-dependent penalty increased by 5 dB when the payload pattern length was increased to  $2^{15} - 1$ . To overcome this limitation, it may be feasible to use Manchester encoding on the payload as this ensures that there are never more than two zeros in a row [12].

We then demonstrated the performance (BER versus received power) of the payload and label, respectively, in three different circumstances. The first case is with just a single labelled channel. The second case is with two channels 100 GHz apart but without any switching of the fast tunable laser. The final case is when the channel being measured is static and the other is switching from the adjacent channel to a distant channel every 260 ns. The laser output is blanked for the first 60 ns of this time. The 60 ns ensures that after coming out of blanking, the laser is always within  $\pm 12.5$  GHz of its target frequency for all channel combinations. A wavelength locking circuit is then activated which holds the output within  $\pm 2.5$  GHz of the target channel after a maximum delay of 200 ns after blanking.

It can be seen that for the payload (Fig. 3(a);  $\triangle$ ,  $\square$ ,  $\diamond$ ), by simply having two channels adjacent to each other, a power penalty of approximately 0.5 dB is introduced due to crosstalk from the label of the adjacent channel. This could be reduced or even eliminated by optimizing the profile of the AWG which is used to select the channels. Further degradation due to the switching of the adjacent channel is negligible. This is the expected behavior because of the wide spacing between the payloads in comparison to any drift of the tunable laser that may occur. For the label (Fig. 3(b);  $\triangle$ ,  $\square$ ,  $\diamond$ ), again the presence of an adjacent channel introduces very little penalty. However, when one of the lasers is switching, an error floor around  $5 \times 10^{-4}$  is introduced due to the label of the switching laser, entering

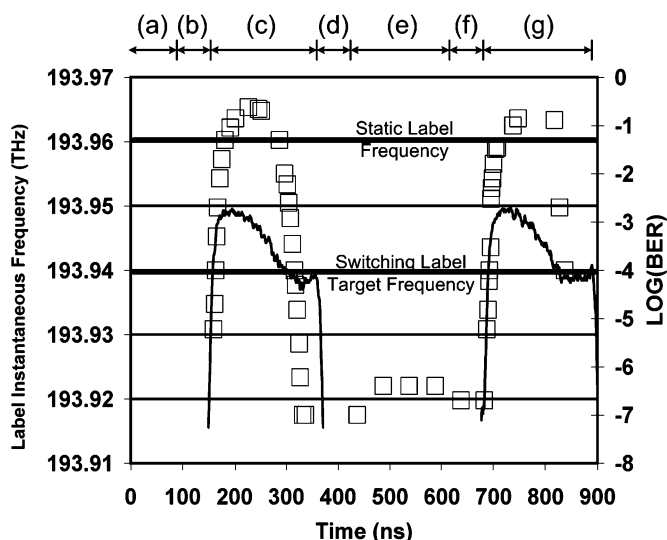


Fig. 4. Time-resolved BER measurements for the extracted label ( $\square$ ) and instantaneous frequency of the switching laser's label. The received power was approximately  $-28.5$  dBm (a) laser at frequency 192.1 THz; (b) laser blanked for 60 ns; (c) laser settling into frequency 193.94 THz for 200 ns; (d) laser blanked for 60 ns; (e) laser at frequency 192.1 THz for 200 ns; (f) laser blanked for 60 ns; (g) laser settling into frequency 193.94 THz for 200 ns.

the filter passband of the measured label. This is caused by the wavelength drift of the tunable laser around its target wavelength. The main cause of this drift after blanking is attributed to the wavelength locking circuit. When this is disabled, although tuning takes longer, the wavelength drift is greatly reduced.

This effect is further illustrated in Fig. 4, which shows time-resolved BER measurements (8-ns gating interval) with a received power of  $-28.5$  dBm along with the instantaneous frequency of the label of the switching laser (extracted from complimentary outputs of the 85-GHz AMZI biased at quadrature for the target frequency). It can clearly be seen that the switching events in the tunable laser correspond to the time intervals when there are significant errors on the received label data. While the laser is blanked and also while it sits at the distant channel, the error rate drops considerably. However, as the laser tunes towards and begins settling on the 193.94-THz channel, the error rate increases dramatically.

While the results presented in this letter are specific to our experiment, there are a number of ways in which the performance of our system and other similar systems can be improved. Clearly the error floor could be minimized by increasing the blanking time and/or channel spacing. However, both of these solutions will reduce network throughput.

More attractive solutions would include optimized channel and label filter profiles, the use of single sideband subcarrier generation to eliminate interference between labels of adjacent channels, and optimization of the transient laser dynamics including operation of wavelength-locking technique during the existing blanking period.

#### IV. CONCLUSION

We have looked at the interference between adjacent wavelength channels in an optical label switched system that employs SCM labels and a duobinary payload. Such a system offers good spectral efficiency, but requires coding to reduce the sensitivity to pattern length. To date, most of the literature on OLS has looked primarily at single-channel systems. We have shown error-free transmission for both payload and label in a two-channel system with 0.4-b/s/Hz spectral efficiency. In addition, we have shown that in WDM systems, severe interference between channels can be caused by wavelength switching effects in tunable lasers that would be used in optical packet transmitters.

#### ACKNOWLEDGMENT

The authors would like to thank the Centre for Integrated Photonics for the loan of the diplexer.

#### REFERENCES

- [1] S. J. B. Yoo, "Optical-packet switching and optical-label switching technologies for the next generation optical internet," in *Proc. Optical Fiber Communications Conf. (OFC 2003)*, 2003, vol. 2, pp. 797–798.
- [2] D. J. Blumenthal, "Photonic packet switching and optical label swapping," *Opt. Netw. Mag.*, pp. 1–12, Nov./Dec. 2003.
- [3] D. Nasset, T. Kelly, and D. Marcenac, "All-optical wavelength conversion using SOA nonlinearities," *IEEE Commun. Mag.*, vol. 36, no. 12, pp. 56–61, Dec. 1998.
- [4] D. J. Blumenthal, "Photonic packet and all-optical label switching technologies and techniques," in *Proc. Optical Fiber Communications Conf. (OFC 2002)*, 2002, pp. 282–284.
- [5] A. Martinez *et al.*, "Experimental demonstration of subcarrier multiplexed optical label swapping featuring 20 GB/s payload speed and 622 Mb/s header conveyed @ 18.3 GHz," in *Proc. 31st Eur. Conf. Optical Communications (ECOC 2005)*, 2005, vol. 4, pp. 959–960.
- [6] M. Y. Jeon, Z. Pan, J. Cao, and S. J. B. Yoo, "BER performance of all optical subcarrier label swapping with 2R regeneration," *IEEE Photon. Technol. Lett.*, vol. 16, no. 1, pp. 323–235, Jan. 2004.
- [7] D. J. Blumenthal, A. Carena, L. Rau, V. Curri, and S. Humphries, "All-optical label swapping with wavelength conversion for WDM-IP networks with subcarrier multiplexed addressing," *IEEE Photon. Technol. Lett.*, vol. 11, no. 11, pp. 1497–1450, Nov. 1999.
- [8] B. Meagher, G. K. Chang, G. Ellinas, Y. M. Lin, W. Xin, T. F. Chen, X. Yang, A. Chowdhury, J. Young, S. J. Yoo, C. Lee, M. Z. Iqbal, T. Robe, H. Dai, Y. J. Chen, and W. I. Way, "Design and implementation of ultra-low latency optical label switching for packet-switched WDM networks," *J. Lightw. Technol.*, vol. 18, no. 12, pp. 1978–1987, Dec. 2000.
- [9] H. J. Lee, S. J. B. Yoo, V. K. Tsui, and S. K. H. Fong, "A simple all-optical label detection and Swapping technique incorporating a fiber Bragg grating filter," *IEEE Photon. Technol. Lett.*, vol. 13, no. 6, pp. 635–637, Jun. 2001.
- [10] J. Buus, M.-C. Amann, and D. J. Blumenthal, "Widely tunable monolithic laser diodes," in *Tunable Laser Diodes and Related Optical Sources*. Hoboken, NJ: Wiley, 2005.
- [11] M. Duelk *et al.*, "Fast packet routing in a 2.5 Tb/s optical switch fabric with 40 Gbit/s duobinary signals at 0.8 b/s/Hz spectral efficiency," in *Proc. Optical Fiber Communications Conf. (OFC 2003)*, 2003, vol. 3, pp. PD8 1–PD8 3.
- [12] J. Zhang, N. Chi, P. V. Holm-Nielsen, C. Peucheret, and P. Jeppesen, "Performance of Manchester-coded payload in an optical FSK labelling scheme," *IEEE Photon. Technol. Lett.*, vol. 15, no. 8, pp. 1174–1176, Aug. 2003.